Differential Stability of Dimeric and Monomeric Cytochrome *c* Oxidase Exposed to Elevated Hydrostatic Pressure†

Jana Staničová,‡ Erik Sedlák,§ Andrej Musatov, and Neal C. Robinson*

Department of Biochemistry, The University of Texas Health Science Center, 7703 Floyd Curl Drive, San Antonio, Texas 78229-3900

Received March 20, 2007; Revised Manuscript Received April 18, 2007

ABSTRACT: Detergent-solubilized dimeric and monomeric cytochrome *c* oxidase (CcO) have significantly different quaternary stability when exposed to 2−3 kbar of hydrostatic pressure. Dimeric, dodecyl maltoside-solubilized cytochrome *c* oxidase is very resistant to elevated hydrostatic pressure with almost no perturbation of its quaternary structure or functional activity after release of pressure. In contrast to the stability of dimeric CcO, 3 kbar of hydrostatic pressure triggers multiple structural and functional alterations within monomeric cytochrome *c* oxidase. The perturbations are either irreversible or slowly reversible since they persist after the release of high pressure. Therefore, standard biochemical analytical procedures could be used to quantify the pressure-induced changes after the release of hydrostatic pressure. The electron transport activity of monomeric cytochrome *c* oxidase decreases by as much as 60% after exposure to 3 kbar of hydrostatic pressure. The irreversible loss of activity occurs in a time- and pressure-dependent manner. Coincident with the activity loss is a sequential dissociation of four subunits as detected by sedimentation velocity, high-performance ion-exchange chromatography, and reversed-phase and SDS−PAGE subunit analysis. Subunits VIa and VIb are the first to dissociate followed by subunits III and VIIa. Removal of subunits VIa and VIb prior to pressurization makes the resulting 11-subunit form of CcO even more sensitive to elevated hydrostatic pressure than monomeric CcO containing all 13 subunits. However, dimeric CcO, in which the association of VIa and VIb is stabilized, is not susceptible to pressure-induced inactivation. We conclude that dissociation of subunit III and/or VIIa must be responsible for pressure-induced inactivation of CcO since VIa and VIb can be removed from monomeric CcO without significant activity loss. These results are the first to clearly demonstrate an important structural role for the dimeric form of cytochrome *c* oxidase, i.e., stabilization of its quaternary structure.

Bovine heart cytochrome *c* oxidase (EC 1.9.3.1, CcO)[1] is the terminal complex of the mitochondrial respiratory chain. It is a multisubunit protein−phospholipid complex consisting of 13 dissimilar subunits, three or four tightly bound cardiolipins, and four metal centers (Cu_A, heme *a*, heme a_3, and Cu_B) with a combined molecular weight of ∼205000 for the monomeric enzyme (*1*−*3*). CcO crystallizes as a dimer, which is generally seen as the functional unit within the inner membrane; however, little or no information is available regarding the functional or structural significance of a dimeric structure. For example, monomeric and dimeric CcO are both highly active in terms of electron transfer (*4*, *5*). The dimeric form of CcO may be required for proton translocation since this activity can be determined experimentally only with dimeric CcO. Monomeric CcO dimerizes during its reconstitution into phospholipid vesicles, precluding assessment of proton translocation with monomeric CcO (*6*, *7*). However, dimerization slows the reduction of catalytic intermediate compound F, suggesting that uptake of protons into the binuclear center is slower with dimeric CcO (*8*).

In this work, elevated hydrostatic pressure was utilized to probe for differential structural and functional stability between monomeric and dimeric CcO. This technique had been used previously only to probe for volume changes associated with conformational switching within detergent-solubilized CcO and to assess the functional role of bound water within the enzyme (*9*−*12*). No attention has been paid to determining the effect of exposure to elevated hydrostatic pressure on either the quaternary protein structure or the electron transport activity. Here, we show that elevated hydrostatic pressure triggers both structural and functional alterations within monomeric cytochrome *c* oxidase, but not within the dimeric enzyme. These results suggest that dimerization may be essential for maintaining the maximum

† This work was supported by grants from the National Institutes of Health (GMS 24795) and The Robert A. Welch Foundation (AQ1481).

* To whom correspondence should be addressed. Telephone: (210) 567-3754. Fax: (210) 567-6595. E-mail: robinson@uthscsa.edu.

‡ Present address: Institute of Chemistry, Biochemistry and Biophysics, University of Veterinary Medicine, Košice, Slovak Republic.

§ Present address: Department of Biochemistry, P. J. Šafárik University, Moyzesova 11, 04154 Košice, Slovak Republic.

[1] Abbreviations: CcO, bovine heart cytochrome *c* oxidase; CcO-A, enzyme containing all 13 subunits; CcO-B, enzyme containing 11 subunits (missing subunits VIa and VIb); CcO-C, enzyme containing 9 subunits (missing subunits III, VIa, VIb, and VIIa); DM, dodecyl maltoside.

10.1021/bi700548a CCC: $37.00
Published on Web 05/26/2007

structural stability of this multisubunit, integral membrane protein complex.

EXPERIMENTAL PROCEDURES

Materials. Dodecyl maltoside was purchased from Anatrace Inc. Sodium cholate and horse heart cytochrome *c* (type III) were purchased from Sigma Chemical Co. The C_{18} reversed-phase HPLC column (4.6 mm × 250 mm, 218TP104, 5 μm, 300 Å pore size) was purchased from Vydac. A HiTrapQ FPLC column (Q Sepharose HP 1 mL) was from Pharmacia Biotech. Other chemicals were analytical grade.

Cytochrome c Oxidase Purification. Bovine heart CcO was isolated from heart muscle particles as previously described (*13*). The final enzyme precipitate was solubilized at ~120 μM heme aa_3 in 0.1 M NaH_2PO_4 buffer (pH 7.4) containing 25 mM sodium cholate and 1.0 mM EDTA and then frozen as ~50 μL aliquots in liquid nitrogen. The purified enzyme contained 9.5−10 nmol of heme A/mg of protein and had a molecular activity of 350−370 s^{-1} when assayed spectrophotometrically with 0.025 M phosphate buffer (pH 7.20) containing 2 mM dodecyl maltoside (DM), with 25−30 μM ferrocytochrome *c* as the substrate.

Preparation of Dimeric, Monomeric, and 11-Subunit Monomeric Cytochrome c Oxidase. CcO dimer, containing two copies of each of the 13 CcO subunits, was prepared by solubilizing ~10 μM CcO in 20 mM Tris-SO_4 buffer (pH 7.4) containing 2 mM DM and 2 mM sodium cholate (*6*). Identical pressurization results were obtained whether sodium cholate was left in the sample or was removed by overnight dialysis against buffer containing only 0.2 mM DM. CcO monomer, containing a single copy of each of the 13 CcO subunits, was prepared by solubilizing ~10 μM CcO in 20 mM Tris-SO_4 buffer (pH 7.4) containing a high concentration of DM, i.e., 10 mM, followed by overnight dialysis against buffer containing 0.2 mM DM (*14*). Formation of CcO dimer and monomer was confirmed by sedimentation velocity analysis as described previously (*6*, *14*). Monomeric CcO containing only 11 subunits, i.e., from which subunits VIa and VIb[2] have been completely removed, was prepared by the HiTrapQ FPLC, anion-exchange chromatography method of Sedlák and Robinson (*18*).

Hydrostatic Pressurization of Cytochrome c Oxidase. Elevated hydrostatic pressure (1−3 kbar)[3] was applied to CcO within a flexible polyethylene high-pressure fluorescence cell (ISS, Inc., Champaign, IL) using an Advanced Pressure Products (Ithaca, NY) liquid pressure generator with ethanol as the pressurizing fluid. The hydrostatic pressure apparatus and fluorometer have been described in detail by Panda et al. (*15*, *16*). The system includes a photon counting spectrofluorometer for measuring the protein fluorescence spectrum during its exposure to high hydrostatic pressure. The temperature was maintained at 25.0 °C with a thermostatically controlled circulating water bath.

Cytochrome c Oxidase Activity Assay. CcO electron transport activity (moles of ferrocytochrome *c* oxidized per mole of CcO per second) was measured spectrophotometrically by following the pseudo-first-order rate of ferrocytochrome *c* oxidation. Enzyme assay conditions were as follows: 1.75 nM CcO, 25−30 μM ferrocytochrome *c*, and 0.025 M phosphate buffer (pH 7.20) containing 2 mM DM (*17*). The effect of high hydrostatic pressure on the activity of CcO was determined immediately (<30 min) after decompression and removal of enzyme from the pressure cell. No significant changes in activity were detected when the enzyme was assayed after 24 h.

HiTrapQ FPLC Anion-Exchange Column Chromatography. Intact CcO and its subunit-depleted subcomplexes were separated by sodium sulfate gradient elution from a HiTrapQ anion-exchange column in Tris-SO_4 buffer (pH 7.4) containing 2 mM DM. The equipment and protocol for the FPLC anion-exchange chromatographic separation of subunit-depleted forms of CcO were described by Sedlák and Robinson (*18*).

Subunit Analysis by Reversed-Phase HPLC and SDS−PAGE. The subunit content of the three HiTrapQ FPLC-purified forms of CcO was quantified by C_{18} reversed-phase HPLC and SDS−PAGE as described previously (*18*, *19*). The 10 nuclear-encoded subunits were quantified using the reversed-phase HPLC method after normalizing each elution peak area assuming a constant yield for subunit Va (association of subunit Va is unaffected by exposure to as much as 3 kbar of hydrostatic pressure). The content of the three mitochondrially encoded subunits was determined after resolution by SDS−PAGE using a 15% acrylamide running gel containing 2 M urea and 0.1% SDS (*19*). The image of the Coomassie Blue G-250-stained gel was captured using a Bio-Rad GS-800 calibrated densitometer and the intensity of each band quantified using NIH ImageJ version 1.37.

Sedimentation Velocity Analysis of Cytochrome c Oxidase. All experiments were conducted in the Center for Analytical Ultracentrifugation of Macromolecular Assemblies located in the Department of Biochemistry at The University of Texas Health Science Center at San Antonio. Sedimentation velocity analysis of CcO was carried out using a Beckman XLA ultracentrifuge at 20 °C and 40 000 rpm using optical absorption detection at 420 nm. The resulting sedimentation velocity data were analyzed according to the method of van Holde and Weischet (*20*) and *C*(*s*) analysis according to the method of Schuck (*21*), both of which were implemented within UltraScan (version 7.1.0). The latter method iteratively fits a single frictional ratio and a distribution of sedimentation coefficients to the sedimentation velocity data. From the best-fit solution, distributions of sedimentation coefficients and diffusion coefficients are obtained. The two coefficients subsequently are used to generate a distribution of molecular weights that are consistent with the sedimenting macromolecules provided they have the same frictional ratio. Sedimentation velocity analysis of detergent-solubilized CcO is complicated by bound detergent (*14*, *22*). The partial specific volume of the protein−detergent complex was used to evaluate the molecular weight of the protein−detergent complex and thus the protein molecular weight, i.e., $s_{20,w}/D_{20,w} = M_{complex}(1 - \bar{\nu}_{complex}\rho_o)/RT$, where $M_{complex} = M_{pr}(1 - \delta_{det})$, $\bar{\nu}_{complex} = (\bar{\nu}_{pr} + \delta_{det}\bar{\nu}_{det})/(1 - \delta_{det})$, and $\delta_{det} = g_{det}/g_{pr}$. The binding of DM to monomeric and dimeric CcO was assumed to be 0.30 g of DM/g of CcO (*14*) and 0.40 g of DM/g of CcO (calculated from the monomer value after correction for the relative surface area of the membrane-spanning portion of CcO).

[2] CcO subunit nomenclature according to Kadenbach et al. (*2*).

[3] Units of pressure: 1 kbar = 1000 bar; 1 bar = 0.1 MPa = 0.987 atm = 14.5 psi.

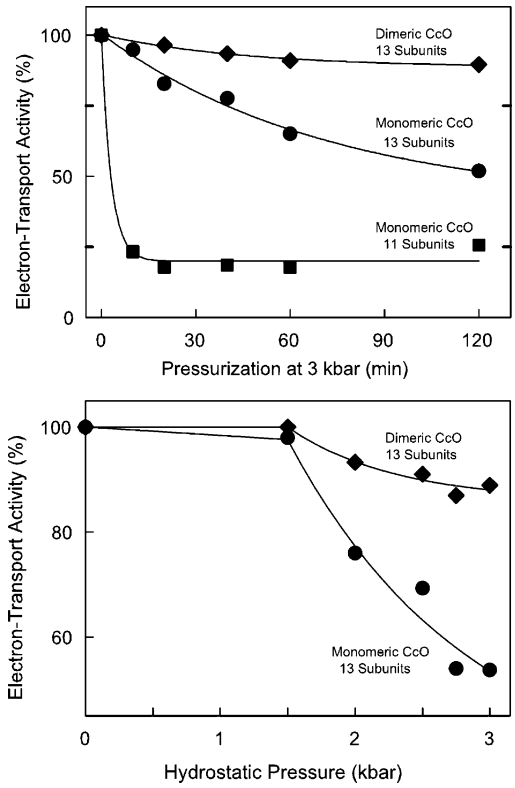

FIGURE 1: Hydrostatic pressure-induced inactivation of cytochrome *c* oxidase. The electron transfer activity of dimeric (◆), 13-subunit monomeric (●), and 11-subunit monomeric CcO (■) was measured as a function of exposure time to 3 kbar of hydrostatic pressure (top) and as a function of hydrostatic pressure treatment for 2 h (bottom). The three data sets were fitted with single-term exponentials. The fitting parameters at infinite time were 88, 40, and 20% for dimeric, monomeric, and 11-subunit CcO, respectively. In each case, 8 μM aa_3 was exposed to hydrostatic pressure at 25 °C in 20 mM Tris-SO_4 buffer (pH 7.4) containing the following amount of detergent: 2 mM DM and 2 mM sodium cholate for dimeric CcO; 10 mM DM for 13-subunit, monomeric CcO; and 2 mM DM for 11-subunit CcO. Electron transfer activity of each sample was measured after decompression and dilution into dodecyl maltoside-containing assay buffer. Data are reproducible to ±5% based upon more than a dozen repetitions of each pressure-induced inactivation curve using four different preparations of CcO.

RESULTS

Inactivation of CcO by Elevated Hydrostatic Pressure. Exposure of monomeric CcO to 2−3 kbar of hydrostatic pressure causes a time- and pressure-dependent loss of enzymatic activity (Figure 1). Pressure-induced inactivation is essentially irreversible since the original activity is not recovered 24 h after CcO is returned to normal atmospheric pressure. The extent of inactivation is highly dependent upon the CcO quaternary structure. Dimeric CcO is quite stable, and 85% of its original activity remains after it has been exposed to 3 kbar of hydrostatic pressure for 2 h. However, monomeric CcO is much more susceptible to pressure-induced inactivation (half of its electron transport activity is lost after exposure to 3 kbar of hydrostatic pressure for 120 min). Monomeric CcO is further destabilized if subunits VIa and VIb are removed prior to the hydrostatic pressure treatment. The monomeric, 11-subunit form of CcO is very sensitive to pressure, and only ∼20% of its enzymatic activity remains after exposure to 3 kbar of hydrostatic pressure for 10 min. Nearly identical inactivation curves were obtained each time monomeric and dimeric CcO were analyzed, including more than a dozen repetitions using four different CcO preparations.

Hydrostatic Pressure-Induced Perturbation of CcO Visible and Fluorescence Spectra. With our equipment, absorbance spectra cannot be collected in "real time" during exposure of CcO to high hydrostatic pressure. Absorbance spectra can only be obtained after decompression and removal of the sample from the pressure cell. Using this approach, no changes are detected in the visible spectrum of monomeric or dimeric CcO after exposure to 3 kbar of pressure for 2 h. Therefore, perturbation of the heme environment is unlikely to be responsible for the pressure-induced inactivation of CcO. Real-time fluorescence spectra can be collected during hydrostatic compression. A small reversible change is detected in the tryptophan fluorescence spectrum of each type of CcO, but this change does not correlate with CcO inactivation. The fluorescence change that occurs with monomeric or dimeric CcO is nearly identical. In each case, exposure to elevated hydrostatic pressure produces an ∼2 nm red shift in the tryptophan emission maximum (em_{max} increases from 328 to 330 nm) with a concomitant 20−25% decrease in the maximum fluorescence intensity, suggesting a slightly increased level of solvent exposure and a decreased fluorescence lifetime for at least some of the 55 tryptophans within CcO. The tryptophan fluorescence spectrum nearly returns to normal immediately upon decompression, with dimeric and monomeric CcO having 96 and 90% of their initial fluorescence intensity, respectively.

Sedimentation Velocity Analysis of CcO after Exposure to Elevated Hydrostatic Pressure. The distribution of sedimentation coefficients ($s_{20,w}$ = 15.5 S) and hydrodynamic mass ($M_w \cong$ 410 000) of dimeric CcO is unaffected by exposure to 3.0 kbar of hydrostatic pressure for 2 h at 25 °C (Figure 2, left two panels). In contrast to those of dimeric CcO, both the hydrodynamic mass and distribution of sedimentation coefficients for monomeric CcO significantly decrease after the CcO is exposed to elevated hydrostatic pressure. Prior to compression, monomeric CcO is nearly homogeneous ($s_{20,w}$ = 11.3 S; $M_{pr} \cong$ 210 000) with less than 5% present as dimers (Figure 2, top right panel). After pressurization to 3 kbar for 2 h, two subcomplexes are generated: ∼35% for which $M_w \cong$ 190 000 and ∼30% for which $M_w \cong$ 150 000 (Figure 2, bottom right panel). Only ∼15% of CcO remains unchanged with $M_w \cong$ 205 000 (small amounts of larger aggregates are also formed). These results suggest that exposure to elevated hydrostatic pressure causes the dissociation of subunits with a combined mass of 10−15 kDa from 35% of the enzyme and 50−60 kDa from another ∼30% of the enzyme.

Resolution of Subunit-Depleted Forms of CcO by Anion-Exchange FPLC. The subunit-depleted forms of CcO can be separated from intact 13-subunit CcO by HiTrapQ anion-exchange column chromatography. Prior to hydrostatic pressure exposure, monomeric and dimeric CcO each elute from HiTrapQ column as one major and one minor chromatographic peak (Figure 3, peaks A and B in left and center panels). With both forms of CcO, enzyme eluting in peak A (∼80−85% of total) contains all 13 CcO subunits, while CcO eluting in peak B (15−20% of total) contains only 11 CcO subunits and is completely devoid of subunits VIa and VIb (Figure 4, trace B, and ref *18*). However, after exposure of monomeric CcO to elevated hydrostatic pressure, a third

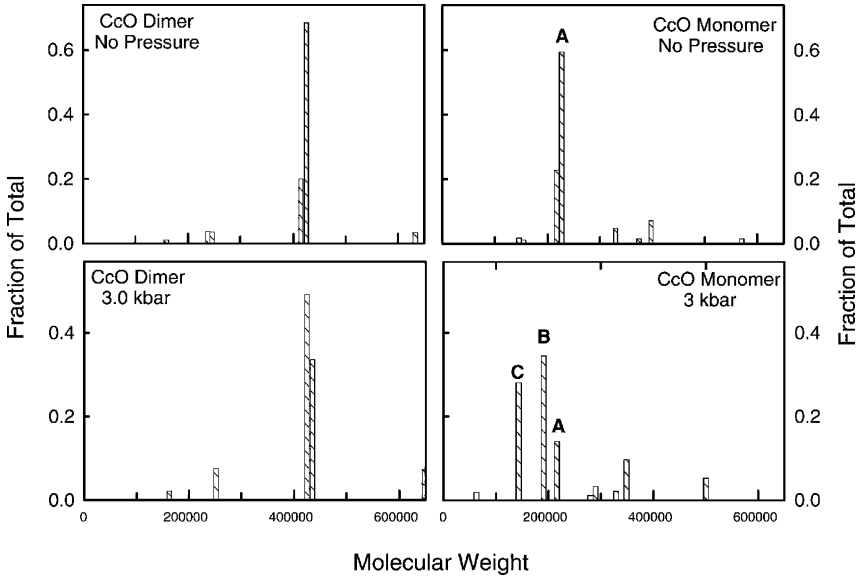

FIGURE 2: Protein molecular weight distributions for dimeric and monomeric CcO before and after exposure to 3 kbar of hydrostatic pressure. In the left panels are protein molecular weight distributions for dimeric CcO before (top) and after (bottom) pressurization at 3 kbar for 2 h. In the right panels are protein molecular mass distributions for 13-subunit monomeric CcO before (top) and after (bottom) pressurization at 3 kbar for 2 h. The histogram bars labeled A, B, and C are CcO subcomplexes for which $M_w \cong 205\,000$, 190 000, 150 000, respectively. Sedimentation velocity data for CcO were acquired at 420 nm during sedimentation at 40 000 rpm. Duplicate samples were analyzed and gave nearly identical results. Data were analyzed by the *C*(*s*) procedure (*21*), which generates a distribution of $s_{20,w}$ and $D_{20,w}$ for each sample based upon a single value for f/f_o. The two coefficients are used to evaluate a distribution of protein molecular weights assuming a constant amount of bound detergent (δ_{det}). The analysis procedure for each CcO sample involved use of the following values for these constants: $\delta_{det} = 0.30$ and $f/f_o = 1.33$ for dimeric CcO before pressurization and $\delta_{det} = 0.30$ and $f/f_o = 1.35$ for dimeric CcO after pressurization; $\delta_{det} = 0.40$ and $f/f_o = 1.31$ for 13-subunit CcO before pressurization and $\delta_{det} = 0.40$ and $f/f_o = 1.20$ for 13-subunit CcO after pressurization. The smaller f/f_o value for monomeric CcO after pressurization most likely was due to the influence of the smaller subcomplexes of CcO. Pressurization conditions were identical to those described in the legend of Figure 1.

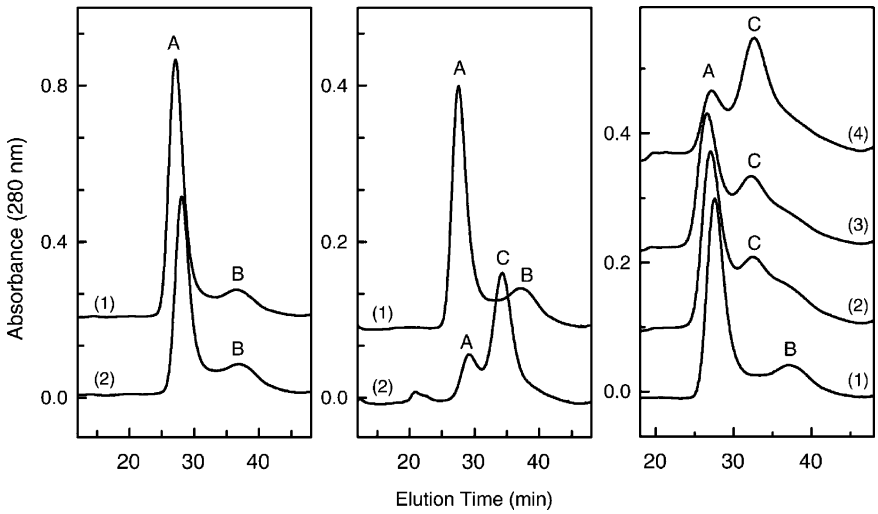

FIGURE 3: Separation of CcO subcomplexes by HiTrapQ FPLC anion-exchange chromatography. The left panel depicts the elution of dimeric CcO before (1) and after (2) pressurization at 3 kbar for 2 h. The middle panel depicts the elution of monomeric CcO before (1) and after (2) pressurization at 3 kbar for 2 h. The right panel depicts the elution of monomeric CcO as a function of time at 3 kbar pressure: (1) 0, (2) 20, (3) 30, and (4) 120 min. Elution and gradient conditions are identical to those previously described (*18*). Nearly identical elution profiles were obtained each time pressure-treated CcO was analyzed (experiment repeated more than a dozen times).

chromatographic species appears (Figure 3, peak C). This pressure-generated form of CcO (peak C) contains only 9 subunits and is devoid of subunits III, VIa, VIb, and VIIa (Figures 4 and 5). The percentage of each CcO form can be quantified as a function of applied hydrostatic pressure by fitting each elution profile to three gaussians (inset of Figure 6). The area under chromatographic peak C (9-subunit form of CcO) increases as a function of the time and magnitude of the applied pressure with a concomitant decrease in chromatographic peak A (intact 13-subunit CcO) (Figure 6, main panel). The conversion of 13-subunit CcO to 9-subunit CcO correlates reasonably well with the loss of enzymatic activity (Figure 6, main panel). The percentage of peak B, i.e., 11-subunit CcO, remains fairly constant before and after pressurization and is presumably a transient intermediate formed during subunit dissociation.

Electron Transport Activity of Intact and Subunit-Depleted CcO. CcO eluting as chromatographic peak C has only 40−45% of the electron transport activity of untreated CcO, while chromatographic peaks A and B are 85−90% of normal

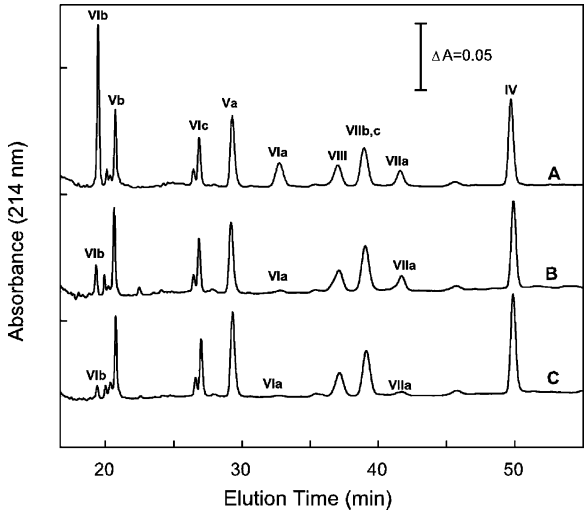

FIGURE 4: Reversed-phase HPLC analysis of nuclear-encoded subunits of CcO and its pressure-generated subcomplexes. Monomeric CcO, after exposure to 3 kbar of hydrostatic pressure for 2 h, was separated by HiTrapQ anion-exchange chromatography into three distinct chromatographic species, i.e., A, B, and C in Figure 3, and the subunit content of each was determined by quantitative reversed-phase HPLC analysis (*27*). Nearly identical subunit compositions were obtained each time the HiTrapQ peaks were analyzed. Data are representative of more than a dozen analyses: (A) subunit content of HiTrapQ peak A, (B) subunit content of HiTrapQ peak B, and (C) subunit content of HiTrapQ peak C. For each analysis, CcO eluting in a HiTrapQ peak was pooled, acidified with 0.2% TFA, and 50−100 μg of protein injected onto the RP-HPLC column.

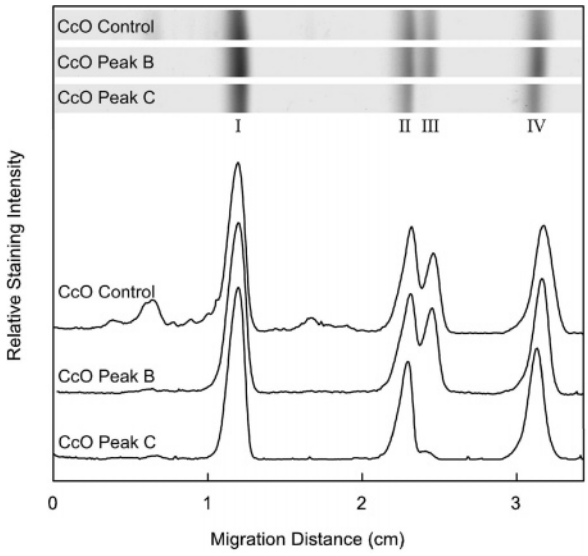

FIGURE 5: SDS−PAGE analysis of mitochondrially encoded subunits of CcO and its pressure-generated subcomplexes. Monomeric CcO, after exposure to 3 kbar of hydrostatic pressure for 2 h, was separated by HiTrapQ anion-exchange chromatography into three distinct chromatographic species, i.e., A, B, and C as described in the legend of Figure 4. The subunit content of CcO eluting in peaks B and C was compared to the subunit content of CcO that had not been exposed to hydrostatic pressure (CcO Control), which is identical to CcO peak A (*27*). The relative amounts of subunits I−IV in each sample were determined by SDS−PAGE using a 15% running gel that contained 2 M urea and 0.1% SDS. Gels were stained, destained, and scanned as described in Experimental Procedures. Data are representative of analyses done in triplicate.

(Table 1). These data suggest that dissociation of subunits III and/or VIIa is responsible for CcO activity loss. In fact, a strong correlation exists between the generation of chro-

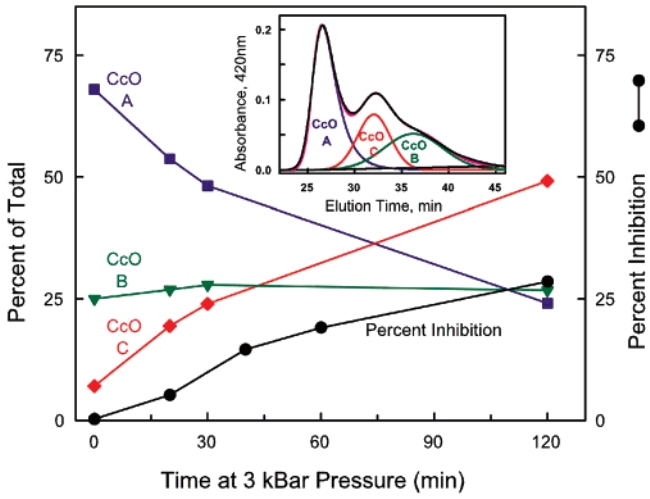

FIGURE 6: Correlation between pressure-induced inactivation of CcO and the generation of a 9-subunit subcomplex of CcO. The relative amounts corresponding to CcO-A (13 subunits), CcO-B (11 subunits), and CcO-C (9 subunits) are plotted in the main figure as a function of pressurization time at 3 kbar. The generation of CcO peak C, i.e., CcO-C containing only 9 subunits (red line), correlates well with the percent loss of enzymatic activity (black line). These data were generated by measuring the electron transfer activity of CcO and the percent of the three forms of CcO, i.e., CcO-A (13 subunits), CcO-B (11 subunits), and CcO-C (9 subunits), as a function of exposure time at 3 kbar of hydrostatic pressure. To obtain the percent CcO-A, CcO-B, and CcO-C, the data depicted in Figure 3 (right panel) were quantified by fitting each elution profile to three slightly skewed gaussians. The inset illustrates such an analysis for the elution of CcO after it was exposed to 3 kbar of hydrostatic pressure for 30 min. The three gaussians fit the original elution profile (black line) very well. The relative amounts corresponding to CcO-A (13 subunits), CcO-B (11 subunits), and CcO-C (9 subunits) were calculated from their respective areas under each gaussian.

Table 1: Electron Transport Activity of Monomeric Control and Pressurized Cytochrome *c* Oxidase[a]

	CcO-A	CcO-B	CcO-C
control	350	340	N/A
2.5 kbar	315	290	147

[a] Activities expressed as micromoles of ferrocytochrome *c* oxidized per micromole of CcO per second. CcO was pressurized at 2.5 kbar for 2 h at 25 °C. CcO, before and after being exposed to hydrostatic pressure, was resolved into CcO-A, CcO-B, and CcO-C with a HiTrapQ anion-exchange column (refer to Figures 3 and 6) and the electron transport activity of each form of CcO measured spectrophotometrically as described in Experimental Procedures. The standard error of the mean for activities was ±3% for control CcO and ±5% for pressurized CcO.

matographic peak C (CcO-C) and CcO inactivation (Figure 6). The activity of CcO-C (43%, Table 1) is also nearly identical to the activity of monomeric CcO exposed to 3 kbar and extrapolated to infinite time (40%, Figure 1). The only inconsistency is the lower activity of 11-subunit CcO after exposure of monomeric CcO to 3 kbar of hydrostatic pressure for 2 h (20%, Figure 1) versus the higher activity of HiTrapQ-purified CcO-C (40%, Table 1). However, these experiments are not directly comparable. The pressure-induced intermediate CcO-B is not identical to the 11-subunit CcO prepared by HiTrapQ chromatography even though both are missing subunits VIa and VIb. The HiTrapQ procedure involves dodecyl maltoside extraction of subunits VIa and VIb, which removes all the bound phospholipid except for

the two cardiolipins near subunit VIIa (*18*, *23*). In contrast, monomeric CcO contains at least four cardiolipins and two to six other phospholipids. The increased sensitivity of the phospholipid-depleted 11-subunit form of CcO could easily be due to its lower phospholipid content. Furthermore, the two samples were not exposed to the same hydrostatic pressure. The data depicted in Figure 1 were collected after exposure of 11-subunit CcO to 3.0 kbar of hydrostatic pressure, while the data listed in Table 1 were obtained after exposure of monomeric CcO to only 2.5 kbar of pressure.

DISCUSSION

Elevated hydrostatic pressure was successfully utilized to probe the functional and structural stability of various oligomeric forms of bovine heart CcO. Dimeric CcO is highly resistant to increased hydrostatic pressure, while monomeric CcO is not. Dimerization must either strengthen subunit interactions within the detergent-solubilized complex or lock the complex into a highly resistant structure. Pressure-induced inactivation is not readily reversible, and the structural perturbations persist hours after decompression. The incomplete recovery of tryptophan fluorescence, the increased $s_{20,w}$ heterogeneity, and loss of enzymatic activity all suggest that the pressure-induced changes in monomeric CcO are effectively irreversible. Because the structural perturbations remain after pressure release, we were able to determine the pressure-induced structural perturbations within the different oligomeric forms of CcO.

Sequential Dissociation of Subunits from Monomeric Cytochrome c Oxidase. Pressure-induced inactivation is not the result of complete disruption of CcO's quaternary structure but occurs together with the progressive dissociation of four subunits: III, VIa, VIb, and VIIa. Dissociation is not random but appears to be highly ordered. The initial rate-limiting step is the dissociation of subunits VIa and VIb followed by the immediate dissociation of subunits VIIa and III. Dissociation of subunits VIa and VIb is not directly linked to pressure-induced inactivation since both subunits can be removed without a significant loss of electron transport activity (*18*). However, enzyme that is missing these two subunits (11-subunit CcO) is much more vulnerable to pressure-induced inactivation (the inactivation rate is ~25-fold faster for 11-subunit CcO than for the 13-subunit form of CcO). The extremely rapid dissociation of subunits III and VIIa when VIa and VIb are no longer present explains the fact that dissociation of VIa and VIb is rate-limiting and why the 11-subunit intermediate does not accumulate during the exposure to elevated hydrostatic pressure. The 11-subunit form is only a transient, kinetic intermediate that disappears as fast as it is produced.

Mechanism for Pressure-Induced Inactivation of Cytochrome c Oxidase. The inactivation and subunit analysis data suggest that dissociation of subunit III and/or VIIa is linked to pressure-induced inactivation. It is not possible to determine whether loss of subunit III or VIIa causes the activity loss. However, genetic removal of subunit III does not alter either the electron transfer or proton translocation activity of *Paracoccus denitrificans* CcO (*24*), suggesting that dissociation of subunit VIIa is responsible for the pressure-induced activity loss. Alternatively, the loss in activity may be due to a pressure-induced structural perturbation in CcO, which indirectly results in the dissociation of both subunits. At present, it is not possible to differentiate between the two possibilities. The subunit VIIa-linked mechanism is intriguing since we previously found that dissociation of subunit VIIa correlates with peroxide-induced inactivation of CcO (*25*). Furthermore, subunit VIIa is involved in the binding of functionally important cardiolipin bound to CcO near the entrance to the D-channel (*26*). Removal of this cardiolipin also decreases the CcO activity. These previous results, together with the findings presented here, indicate subunit VIIa has a critical function in CcO.

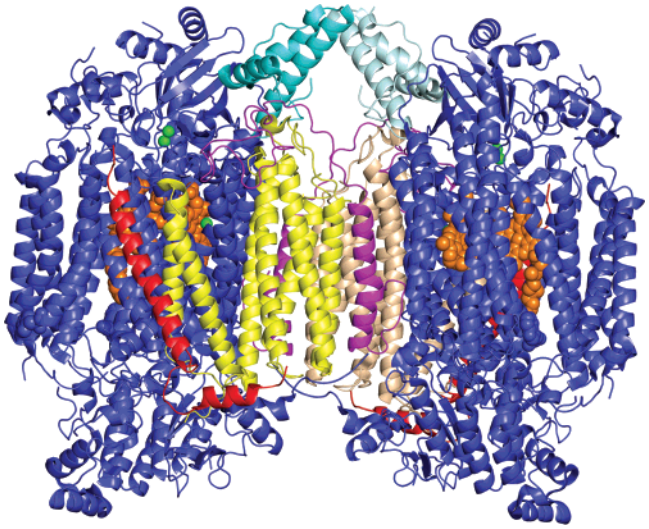

FIGURE 7: Three-dimensional structure of dimeric CcO illustrating the location of the four subunits that dissociate during exposure to hydrostatic pressure: yellow and tan for subunit III, magenta for subunit VIa, light and dark teal for subunit VIb, red for subunit VIIa, orange for heme *a* and a_3, and green for Cu_A and Cu_B. All other subunits are colored blue. Subunits VIa and VIb are the first subunits to dissociate during pressurization of CcO. In the CcO dimer, both of these subunits are "trapped" at the dimer interface, preventing their dissociation. In monomeric CcO, this constraint is removed, enabling both subunits to dissociate and produce CcO-B, an 11-subunit complex of CcO. Subsequent to the dissociation of subunits VIa and VIb is the dissociation of subunits III and VIIa. Subunit III is located at the dimer interface, and its association is also stabilized by CcO dimerization. This figure was prepared using PyMol (DeLano Scientific LLC, San Francisco, CA) using atomic coordinates of CcO [PDB entry 1v54 (*1*)].

Structural Stability of Dimeric Cytochrome c Oxidase. Dimeric CcO is structurally and functionally highly resistant to pressures up to 3 kbar. The small loss of activity (<15%) induced during exposure of dimeric CcO to elevated hydrostatic pressure is almost certainly due to complete inactivation of the small amount of monomeric CcO (10−15%) that is always present in our dimeric CcO preparations (refer to Figures 2 and 3). This unavoidable structural heterogeneity almost certainly explains the small but reproducible pressure-induced inactivation of dimeric CcO.

The strong resistance of dimeric CcO to pressure-induced inactivation reinforces our conclusion that dissociation of subunits VIa and VIb precedes CcO inactivation. Both subunits are located at the dimer interface and stabilize dimeric CcO by forming the major contacts between the two monomers (Figure 7). If subunits VIa and VIb stabilize dimeric CcO, then dimerization must stabilize the association of subunits VIa and VIb and decrease their susceptibility to pressure-induced dissociation. Since dissociation of subunits

VIa and VIb must occur prior to loss of activity, dimerization of CcO effectively protects it from inactivation.

We, therefore, conclude that (1) dissociation of subunits from CcO is an ordered process, i.e., VIa and VIb dissociate first followed immediately by the dissociation of VIIa and III, (2) dissociation of subunits VIIa and III coincides with pressure-induced inactivation of CcO, and (3) dimerization stabilizes the association of VIa and VIb and, therefore, the functional integrity and entire quaternary structure of CcO. These findings are the first clear demonstration that dimeric CcO has an important structural role, i.e., stabilization of its quaternary structure against environmental perturbations.

ACKNOWLEDGMENT

We thank Dr. Markandeswar Panda for his instruction on the use of the pressurization equipment, Tiffany McDonald-Marsh for her technical assistance, and Dr. LeAnn K. Robinson for her editorial help in preparing the manuscript.

REFERENCES

1. Tsukihara, T., Aoyama, H., Yamashita, E., Tomizaki, T., Yamaguchi, H., Shinzawa-Itoh, K., Nakashima, R., Yaono, R., and Yoshikawa, S. (1996) The whole structure of the 13-subunit oxidized cytochrome *c* oxidase at 2.8 Å, *Science 272*, 1136−1144.
2. Kadenbach, B., Jarausch, J., Hartmann, R., and Merle, P. (1983) Separation of mammalian cytochrome *c* oxidase into 13 polypeptides by sodium dodecyl sulfate-gel electrophoresis procedure, *Anal. Biochem. 129*, 517−521.
3. Robinson, N. C. (1993) Functional binding of cardiolipin to cytochrome *c* oxidase, *J. Bioenerg. Biomembr. 25*, 153−163.
4. Suarez, M. D., Revzin, A., Narlock, R., Kempner, E. S., Thompson, D. A., and Ferguson-Miller, S. (1984) The functional and physical form of mammalian cytochrome *c* oxidase determined by gel filtration, radiation inactivation, and sedimentation equilibrium analysis, *J. Biol. Chem. 259*, 13791−13799.
5. Robinson, N. C., and Talbert, L. (1986) Triton X-100 induced dissociation of beef heart cytochrome *c* oxidase into monomers, *Biochemistry 25*, 2328−2335.
6. Musatov, A., and Robinson, N. C. (2002) Cholate-induced dimerization of detergent- or phospholipid-solubilized bovine cytochrome *c* oxidase, *Biochemistry 41*, 4371−4376.
7. Estey, L. A., and Prochaska, L. J. (1993) Detection of bovine heart mitochondrial cytochrome *c* oxidase dimers in Triton X-100 and phospholipid vesicles by chemical cross-linking, *Biochemistry 32*, 13270−13276.
8. Sadoski, R. C., Zaslavsky, D., Gennis, R. B., Durham, B., and Millet, F. (2001) Exposure of bovine cytochrome *c* oxidase to high Triton X-100 or to alkaline conditions causes a dramatic changes in the rate of reduction of compound F, *J. Biol. Chem. 276*, 33616−33620.
9. Kornblatt, J. A., and Hui Bon Hoa, G. (1982) Conformations of cytochrome *c* oxidase: Thermodynamic evaluation of the interconversion of the 418- and 428-nm forms, *Biochemistry 21*, 5439−5444
10. Kornblatt, J. A., Hui Bon Hoa, G., and English, A. M. (1984) Volume changes associated with cytochrome *c* oxidase-porphyrin cytochrome *c* equilibrium, *Biochemistry 23*, 5906−5911
11. Kornblatt, J. A., Hui Bon Hoa, G., and Heremans K. (1988) Pressure-induced effects on cytochrome *c* oxidase: The aerobic steady state, *Biochemistry 27*, 5122−5128.
12. Kornblatt, J. A., and Hui Bon Hoa, G. (1990) A nontraditional role for water in the cytochrome *c* oxidase reaction, *Biochemistry 29*, 9370−9376.
13. Mahapatro, S. N., and Robinson, N. C. (1990) Effect of changing the detergent bound to bovine cytochrome *c* oxidase upon its individual electron-transfer steps, *Biochemistry 29*, 764−770.
14. Musatov, A., Ortega-Lopez, J., and Robinson, N. C. (2000) Detergent-solubilized bovine cytochrome *c* oxidase: Dimerization depends upon the amphiphilic environment, *Biochemistry 39*, 12996−13004.
15. Panda, M., Ybarra, J., and Horowitz, P. M. (2001) High hydrostatic pressure can probe the effects of functionally related ligands on the quaternary structures of the chaperonins GroEL and GroES, *J. Biol. Chem. 276*, 6253−6259.
16. Panda, M., and Horowitz, P. M. (2002) Conformational heterogeneity is revealed in the dissociation of the oligomeric chaperonin GroEL by high hydrostatic pressure, *Biochemistry 41*, 1869−1876.
17. Dale, M. P., and Robinson, N. C. (1988) Synthesis of cardiolipin derivatives with protection of the free hydroxyl: Its application to the study of cardiolipin stimulation of cytochrome *c* oxidase, *Biochemistry 27*, 8270−8275.
18. Sedlák, E., and Robinson, N. C. (1999) Phospholipase A_2 digestion of cardiolipin bound to bovine cytochrome *c* oxidase alters both activity and quaternary structure, *Biochemistry 38*, 14966−14972.
19. Robinson, N. C., Strey, F., and Talbert, L. (1980) Investigation of the essential boundary layers phospholipids of cytochrome c oxidase using Triton X-100, *Biochemistry 19*, 3656−3661.
20. Van Holde, K. E., and Weischet, W. O. (1978) Boundary analysis of sedimentation-velocity experiments with monodisperse and polydisperse solutes, *Biopolymers 17*, 1387−1403.
21. Schuck, P. (2000) Size distribution analysis of macromolecules by sedimentation velocity ultracentrifugation and Lamm equation modeling, *Biophys. J. 78*, 1606−1619.
22. Robinson, N. C., Gomez, B., and Musatov, A. (1998) Analysis of Detergent-Solubilized Membrane Proteins in the Analytical Ultracentrifuge, *Chemtracts: Biochem. Mol. Biol. 11*, 980−968.
23. Sedlák, E., Panda, M., Dale, M. P., Weintraub, S. T., and Robinson, N. C. (2006) Photolabeling of cardiolipin binding subunits within bovine heart cytochrome *c* oxidase, *Biochemistry 45*, 746−754.
24. Haltia, T., Saraste, M., and Wikström, M. (1991) Subunit III of cytochrome c oxidase is not involved in proton translocation: A site-directed mutagenesis study, *EMBO J. 10*, 2015−2021.
25. Musatov, A., Hebert, E., Carroll, C. A., Weintraub, S. T., and Robinson, N. C. (2004) Specific modification of two tryptophans within the nuclear-encoded subunits of bovine cytochrome *c* oxidase by hydrogen peroxide, *Biochemistry 43*, 1003−1009.
26. Sedlák, E., Panda, M., Dale, M. P., Weintraub, S. T., and Robinson, N. C. (2006) Photolabeling of cardiolipin binding subunits within bovine heart cytochrome *c* oxidase, *Biochemistry 45*, 746−754.
27. Liu, Y.-C., Sowdal, L., and Robinson, N. C. (1995) Separation and quantitation of cytochrome *c* oxidase subunits by mono Q fast liquid chromatography and C18 reverse phase HPLC, *Arch. Biochem. Biophys. 324*, 135−142.

BI700548A